BJR https://doi.org/10.1259/bjr.20210310

Received: 08 March 2021 | Revised: 06 July 2021 | Accepted: 12 July 2021

Cite this article as:
Kousi E, Messiou C, Miah A, Orton M, Haas R, Thway K, et al. Descriptive analysis of MRI functional changes occurring during reduced dose radiotherapy for myxoid liposarcomas. *Br J Radiol* 2021; **94**: 20210310.

FULL PAPER

Descriptive analysis of MRI functional changes occurring during reduced dose radiotherapy for myxoid liposarcomas

[1]EVANTHIA KOUSI, [2]CHRISTINA MESSIOU, [3]AISHA MIAH, [1]MATTHEW ORTON, [4,5]RICK HAAS, [6]KHIN THWAY, [1]GEORGINA HOPKINSON, [3]SHANE ZAIDI, [3]MYLES SMITH, [3]ELIZABETH BARQUIN, [2]ELEANOR MOSKOVIC, [7]NICOS FOTIADIS, [8]DIRK STRAUSS, [8]ANDREW HAYES and [1]MARIA A SCHMIDT

[1]MRI unit, The Royal Marsden NHS Foundation Trust and The Institute of Cancer Research, London, UK
[2]Radiology department, The Royal Marsden NHS Foundation Trust, London, UK
[3]Sarcoma Unit, The Royal Marsden NHS Foundation Trust, London, UK
[4]Sarcoma Unit, Department of Radiotherapy, The Netherlands Cancer Institute, Amsterdam, The Netherlands
[5]Department of Radiotherapy, Leiden University Medical Center, Leiden, The Netherlands
[6]Molecular pathology, The Royal Marsden NHS Foundation Trust, London, UK
[7]Department of Interventional Radiology, The Royal Marsden NHS Foundation trust, London, UK
[8]Sarcoma/Melanoma Unit, The Royal Marsden NHS Foundation Trust, London, UK

Address correspondence to: Dr Evanthia Kousi
E-mail: *ekousi@icr.ac.uk*

Objectives: Myxoid liposarcomas (MLS) show enhanced response to radiotherapy due to their distinctive vascular pattern and therefore could be effectively treated with lower radiation doses. This is a descriptive study to explore the use of functional MRI to identify response in a uniform cohort of MLS patients treated with reduced dose radiotherapy

Methods: 10 patients with MLS were imaged pre-, during, and post-radiotherapy receiving reduced dose radiotherapy and the response to treatment was histopathologically assessed post-radiotherapy. Apparent diffusion coefficient (ADC), T2* relaxation time, volume transfer constant (Ktrans), initial area under the gadolinium curve over 60 s (IAUGC60) and (Gd) were estimated for a central tumour volume.

Results: All parameters showed large inter- and intra-subject variabilities. Pre-treatment (Gd), IAUGC60 and Ktrans were significantly different between responders and non-responders. Post-radiotherapy reductions from baseline were demonstrated for T2*, (Gd), IAUGC60 and Ktrans for responders. No statistically significant ADC differences were demonstrated between the two response groups. Significantly greater early tumour volume reductions were observed for responders.

Conclusions: MLS are heterogenous lesions, characterised by a slow gradual contrast-agent uptake. Pre-treatment vascular parameters, early changes to tumour volume, vascular parameters and T2* have potential in identifying response to treatment. The delayed (Gd) is a suitable descriptive parameter, relying simply on T1 measurements. Volume changes precede changes in MLS functionality and could be used to identify early response.

Advances in knowledge: MLS are are characterised by slow gradual contrast-agent uptake. Measurement of the delayed contrast-agent uptake (Gd) is simple to implement and able to discriminate response.

INTRODUCTION

Soft tissue sarcomas (STS) represent a heterogeneous group of approximately 50 histological subtypes. Although in general sarcomas are considered to be radioresistant, studies suggest that myxoid liposarcomas (MLS) may show improved response rates following radiotherapy (RT) than other types of STS. A marked volume decrease, necrosis, and high control rates have been reported after a standardised pre-operative RT protocol (25 × 2 Gy).[1–4] The reason for this remarkable clinicopathological response is unknown but it is hypothesised that damage to the distinctive vascular pattern of MLS is a mechanism that may be relevant to radiosensitivity.[2]

Targeting tumour vasculature with lower than the standard dose levels could prove equally effective[5–7]; permanent radiation-induced damage to vascular endothelium and structure has been reported from doses as low as 10 Gy.[5–8]

The Dose Reduction of Preoperative Radiotherapy in Myxoid Liposarcomas (DOREMY) multicentre clinical trial aimed to investigate whether MLS can be effectively and safely treated with lower doses of radiation pre-operatively. The recently published results show that a treatment dose of 36 Gy achieved excellent local control rate (100%) and reduced wound complication rate (17%) providing an acceptable alternative for pre-operative radiotherapy in MLS.[9]

MRI is a particularly useful modality for the evaluation of STS, however, conventional MRI alone has a limited efficacy for assessing treatment-related response accurately when pathologic post-treatment changes share similar imaging characteristics with viable tumour.[10,11] In clinical trials, volumetric measurements at MRI are commonly used to evaluate tumour response, however, poor correlations with patient outcomes have been demonstrated in heterogeneous patient cohorts.[12,13]

Changes in perfusion, cell proliferation and hypoxia often precede tumour size and morphologic alterations, and quantitative functional MR imaging techniques such as diffusion-weighted imaging (DWI), dynamic contrast-enhanced MRI (DCE-MRI) and T2* imaging are increasingly used to detect early changes.[14–16] Reports on the pre-operative therapeutic monitoring of STS using functional MRI are limited in the literature. Few studies have demonstrated significant reductions in model-based kinetic parameters as early as 2 weeks after treatment initiation[17,18] and quantitative DWI has shown promise to identify early response to treatment for STS.[19] Given the histologic diversity of STS before and after treatment,[2,13] measuring T2* may become relevant in monitoring treatment response[20] but the value of T2* as a prognostic factor of STS response, has not been explored. To date, functional MRI has not been applied specifically to MLS.

This is a pilot study which aims to describe early and late changes in tumour function in a cohort of patients with MLS receiving reduced dose RT pre-operatively and explore the use of MRI functional parameters to identify response. This cohort comprises a subset of patients from the DOREMY clinical trial. All patients were scanned employing a quantitative MRI protocol which was developed in one of the nine tertiary centres involved in the trial.

METHODS AND MATERIALS

10 patients (5 males, 5 females, median age = 41.5 years, age range = 21–53 years) with histologically confirmed MLS were scanned at 3T (Skyra, Siemens Medical Systems, Erlangen, Germany). The tumours were located in the thigh (n = 9) and gluteal (n = 1) regions. All scans were performed with the approval of the research ethics committee (REC reference number: 14/WA/1090).

Treatment protocol

Conformal RT or intensity-modulated RT were planned to deliver 36 Gy in 18 fractions, in daily fraction of 2 Gy, 5 days per week for an overall treatment time of 3.5–4 weeks.[9]

Repeated ultrasound-guided biopsies were performed on fractions 8 and 16 to assess the extent of tumour pathology changes (percentage viable cells, hyalinisation, proliferation and necrosis in proportion of viable cells) and alteration of vasculature. After the last (18th) fraction of 2 Gy patients were followed for 4–6 weeks before they underwent the definitive surgical resection. Tumour excision and the final histopathological assessment were performed 6–8 weeks post-RT, and used to assess response to treatment.

MR imaging protocol

MR imaging was performed pre-RT (visit 1), during RT at fractions 8 (visit 2) and 16 (visit 3), 4 weeks post-RT (visit 4) and 6 weeks post-RT (visit 5). For 2/10 patients, the final MRI visit was at 4 weeks post-RT (visit 4) for logistical purposes. The final MRI visit (the visit closer to the tumour excision) will be denoted as post-RT visit.

All patients were carefully positioned following the RT treatment set-up position. Table 1 details the imaging acquisition protocol.

Data post-processing and analysis

MR image processing and analysis were performed in MATLAB R2018b (The MathWorks, Inc., Natick, MA) and IDL (IDL 8.4, Boulder, CO). When necessary, non-rigid registration performed to compensate for patient movement and muscle deformation (MIRT – Medical Image Registration Toolbox, MATLAB, R2018b).[21] High resolution DIXON at pre- and post-contrast and DWI data sets were aligned to the 2D multiecho GRE and DCE data sets and were resampled to match their spatial resolution (1.5 × 1.5 × 3 mm).

A pre-requisite in quantitative DCE-MRI is to ensure accurate pre-contrast variable flip angle (VFA) T1 measurements which are susceptible to errors due to spatial variations in flip angle caused by RF field (B1) inhomogeneity and are more pronounced at large field-of-views (FOVs) and higher magnetic field strengths (≥3T).[22] Fat-only images from the 2-point Dixon GRE acquisitions for DCE-MRI were employed to correct the nominal flip angles. Flip-angle scaling factors were estimated for each voxel using fat (T1 = 370 ms at 3T) as the reference signal and interpolated (Delaunay triangulation, IDL) over the entire area of interest.[23] The mean scaling factor was then calculated for the lesion only and applied to correct the nominal flip angle values used for pharmacokinetic analysis (Figure 1). For each patient, the median and the median absolute deviation of tumour ADC, T2* relaxation time, gadolinium concentration (Gd), initial area under the gadolinium curve over 60 s ($IAUGC_{60}$) and volume transfer constant (K^{trans}) maps were calculated over five central slices using in-house software (IDL applications - ADEPT and MRIW, The Institute of Cancer Research, UK), for visits 1 (pre-RT) and 2 (RT fraction 8) and for the final post-RT visit (visit 5 for 8/10 and visit 4 for 2/10 patients.

ADC and T2* were measured voxelwise employing Levenberg-Marquardt least-squares monoexponential fits. The K^{trans} model parameter was estimated for all the enhancing voxels using the Tofts-Kety two-compartment model[24] along with

Table 1. Image acquisition protocol

	TR/TE (ms)	Voxel size (mm^3)	Acquisition matrix	Reconstruction matrix	Receiver bandwidth Hz/px	Flip angle	b-values (s/mm^2)	Tumour coverage
Pre-contrast								
High resolution 2-point 3D GRE DIXON	7/3.69	1.25 × 1.25×2	192 × 154	192 × 192	605	four °/16°	N/A	Full
DW-EPI	11200/77	1 × 1×4	128 × 104	208 × 256	2055	90°	50, 300, 600, 900	Full
2D multi echo GRE	100/10 echo times (range 4.9–68.9)	1.5 × 1.5×3	160 × 160	160 × 160	490	45	N/A	Central volume
Post-contrast								
DCE-MRI 2-point 3D GRE DIXON	5.74/2.46	1.5 × 1.5×3	160 × 141	160 × 160	600	four °/16°	N/A	Central volume
High resolution 2-point 3D GRE DIXON	7/3.69	1.25 × 1.25×2	192 × 154	192 × 192	605	four °/16°	N/A	Full

DCE-MRI, Dynamic contrast enhanced-MRI; DW-EPI, diffusion weighted echoplanar imaging; GRE, Gradient echo.
DWI, 2D multiecho GRE and DCE-MRI sequences were centered on a slice chosen by a specialist sarcoma radiologist to ensure targetingthe section of the tumour with increased cellularity and to avoid areas of high fat content.
DCE-MRI comprised 85 dynamic acquisitions with time resolution 3 s with the highest flip angle (16°) [a gadolinium based contrast administration (2 ml s^{-1} followed by 20 ml saline flush)]

population-averaged arterial input function (AIF).[25,26] A population-based AIF has been recommended for improved Ktrans repeatability and treatment sensitivity.[27] The values were adjusted to incorporate changes in the enhancing fraction (EF) of the tumour as in.[28] Voxels of non-convergence of the model or exhibiting no enhancement were removed when estimating tumour K^{trans}.

The concentration of the contrast agent ((Gd)) in each voxel was calculated quantitatively from T_1 values acquired from the downsampled, 2-point 3D gradient echo (GRE) based Dixon sequences before and after contrast administration. The T1 values were calculated using the variable flip angle method and (Gd) measurements were made after DCE corresponding to late enhancement.

Figure 1. Flip angle correction using the signal ratio of two fat-only Dixon images (a, b). The fat is segmented (c) and the corresponding image ratio is interpolated over the entire area (d) to construct the flip angle scaling map (f). The tumour is delineated on a post-contrast frame (e), and the mean scaling factor is derived.

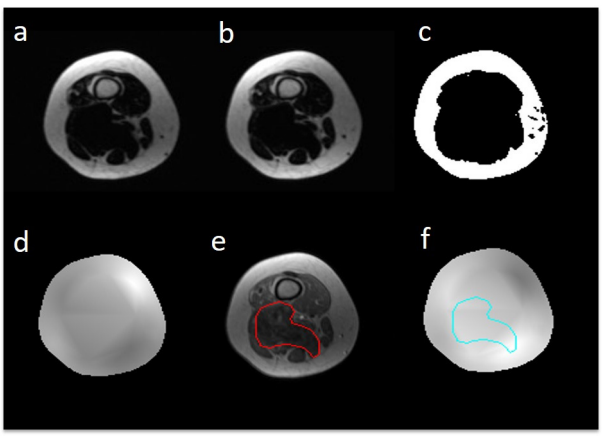

Tumours were delineated on subtracted images derived from the DCE data sets and the regions of interest (ROIs) were transferred to the corresponding parametric maps and combined to a volume of interest (VOI). The tumour volume within the VOI was also estimated from the volume of all voxels included in the VOI.

Descriptive statistics were computed to summarise all metrics from visits 1 (pre-RT), 2 (RT fraction 8) and from the final post-RT visit before tumour excision to explore early and late tumour functional changes within the course of RT. Differences between responders and non-responders were assessed using two-sided Wilcoxon rank sum tests. The percent changes relative to baseline (visit 1) were also reported and the relations between different metrics were investigated using Pearson's product–moment correlation coefficient. For all statistical tests $p < 0.05$ was considered significant. Due to the small sample size, type II errors are more likely to occur and therefore no corrections for multiple testing were applied.

In this article, patients were classified as responders and non-responders according to their final histopathological assessment only: patients with 10% (or less) viable tumour were classified as responders. This stringent response criterion was employed in the run-in period of this trial to ensure patient safety in a dose reduction study. For completeness, the radiotherapy response was also assessed using the response evaluation criterion in solid tumors (v. 1.1) (RECIST 1.1)[29] comparing pre- and post- treatment T_2 weighted images.

RESULTS

Five patients were evaluated as having stable disease and five as partial responders by RESICST 1.1 criteria comparing the pre- and post– treatment T_2 weighted images. Six patients were classified as responders and four as non-responders based on their final histopathological assessment.

Figure 2. Pre- and post-contrast in-phase and pre-contrast fat-only DIXON-based images show the imaging and enhancement variability in our cohort.

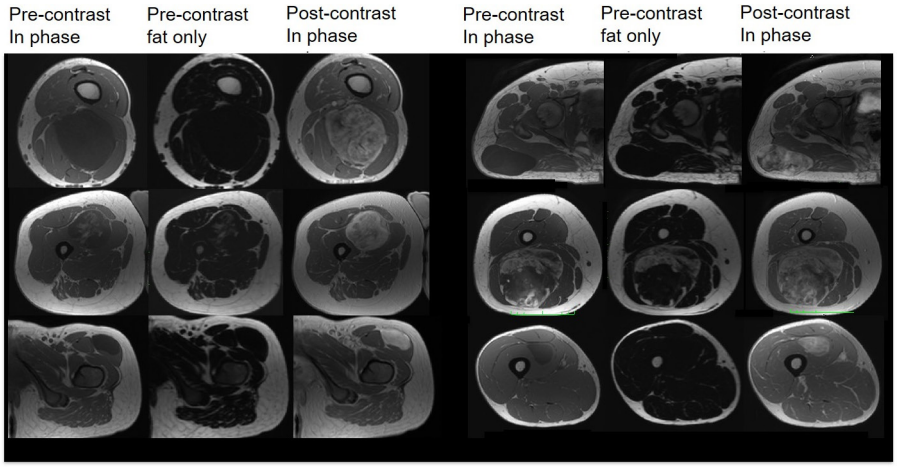

Mean ± standard deviation of the maximum axial tumour dimensions at pre- and post-treatment is 89.8 ± 58.7 (range: 231–30) and 62.5 ± 40.4 (148–20) respectively.

Appearance of MLS at pre-treatment MRI

All MLS masses considered in our cohort were well-defined. On the non-enhanced T_1 weighted Dixon-based in-phase images (Figure 2, first row), the majority of the tumours appeared homogeneous and exhibited low signal intensities, due to the predominant myxoid component. High signal intensity foci within a low signal intensity mass in 2/10 MLS (Figure 2, second row) corresponded to the fat content of these tumours revealed in the final histopathological assessment.

One patient was contraindicated for gadolinium-based contrast agent on all MRI visits. The enhancement pattern of MLS was mostly heterogeneous as in Figure 2 (first and second rows) showing a gradual increase in enhancement following contrast administration (Supplementary Figure 1). In 2/9 patients who received gadolinium, tumours exhibited a homogeneous contrast uptake (Figure 2, third row).

MRI parameters and post-treatment changes

Table 2 summarises the mean ± standard deviation of the median MRI metrics of all the tumour volumes considered for responders and non-responders at baseline (visit 1), visit 2 and the post-RT visit. The use of a flip angle scaling factor (0.97 ± 0.16, mean ± standard deviation, range 0.61–1.26) enabled a larger number of voxels to be successfully modelled. Slow gradual contrast-agent uptake described by very low K^{trans} values. It was impossible to estimate K^{trans} for one patient in the responders group, as the two compartment model was a poor fit for the data, and therefore, this tumour was excluded from the pharmacokinetic analysis.

Large standard deviations of parameter estimates indicate large intersubject variability in the cohort. Comparisons showed significant differences between responders and non-responders at baseline (Gd), IAUGC60 and K^{trans} ($p = 0.024$, 0.024. 0.036, Table 2), but

Table 2. Mean ± standard deviation of the median values obtained from the tumour volumes for responders and non-responders

MRI parameters	Responders ($n = 6$)			Non-responders ($n = 4$)		
	Visit 1	Visit 2	Post-RT visit	Visit 1	Visit 2	Post-RT visit
ADC (x10-5 mm2/s)	229.3 ± 47.9	251.8 ± 24.3	238.6 ± 27.7	227.2 ± 27.7	246.2 ± 29.8	193.7 ± 51.8
T2[a] (ms)	163.6 ± 75.7	145.9 ± 86.4	58.0 ± 25.0	64.2 ± 54.8	63.7 ± 47.0	33.8 ± 17.9
(Gd) ([a]10–3 mmol ml^{-1})	0.5 ± 0.2[a]	0.42 ± 0.22	0.16 ± 0.13	0.09 ± 0.05[a]	0.14 ± 0.08	0.10 ± 0.03
IAUGC (mmol*s)	7.5 ± 3.0[a]	7.0 ± 5.0	3.7 ± 2.1	1.8 ± 1.1[a]	3.1 ± 0.9	3.3 ± 1.1
K^{trans} (min-1) (adjusted to EF)	0.07 ± 0.02[a]	0.06 ± 0.04	0.04 ± 0.03	0.02 ± 0.01[a]	0.03 ± 0.01	0.03 ± 0.01
Volume (cc)	54.3 ± 40.8	43.3 ± 33.2	23.8 ± 19.7	64.7 ± 58.7	65.0 ± 60.0	40.5 ± 40.0
RECIST 1.1 response classification[b]	Partial response ($n = 4$) Stable disease ($n = 2$)			Partial response ($n = 1$) Stable disease ($n = 3$)		

ADC, apparent diffusion coefficient; RT, radiotherapy.

Response classification according to RECIST 1.1 criteria. Number of patients considered for the calculations are clearly stated in the legend of Figure 3.

[a]Denotes significant differences between responders and non-responders.

[b]Please see Supplementary Table 1 for the RECIST 1.1 classification of all 10 patients separately.

Table 3. % change of the mean between baseline, visits two and post-RT for responders and non-responders

MRI parameter	Responders		Non-responders	
	Visit 1/2 % change	Visit 1/post-RT visit % change	Visit 1/2 % change	Visit 1/post-RT visit % change
ADC (x10-5 mm2/s)	9.8	4.1	8.4	−14.8
T2[a] (ms)	−10.8	−64.5[a]	−0.8	−47.4
(Gd) ([a]10–3 mmol ml^{-1})	−7.9	−64.2[a, b]	67.7	13.2[b]
IAUGC60 (mmol*s)	−6.9	−50.8[a, b]	69.8	77.2[b]
K^{trans} (min-1)	−18.5	−48.3[a, b]	47.6	61.8b
Volume (cc)	−20.2b	−56.2	0.6b	−37.3

ADC, apparent diffusion coefficient.
[a]Denotes significant differences between parameters at baseline and the post-RT visit.
[b]Denotes significant differences in parameters changes between responders and non-responders.

no differences were observed for visit 2 and at the post-RT visit. At baseline, responders exhibited higher tumoral T2* values than non-responders, however, this difference was not statistically significant.

Table 3 lists the % change of all the parameter means for visit 2 and the post-RT visit when compared to baseline. In the responders group, statistically significant reductions of post-RT T2*, (Gd), IAUGC60 and K^{trans} were demonstrated (p = 0.004, 0.015, 0.026, 0.030 respectively) when compared to the baseline values. On the contrary, all post-RT vascular parameters in the non-responders group increased and the changes from baseline were significantly different from responders [p = 0.048, 0.048, 0.036 for (Gd), IAUGC60 and K^{trans} respectively]. There were significantly greater decreases in tumour volume in responders compared to non-responders after eight fractions (visit 2) (p = 0.038); non-responders exhibited smaller tumour volume reductions than responders post-RT but the difference was not significant.

The graphs in Figure 3 show the median parameter estimates and the corresponding median absolute deviation at visit 1, visit 2 and the post-RT visit. Considering patients individually, all tumours exhibited early ADC increases. For 3/6 responders, the ADC values further increased post-RT (Figure 3a) and 2 of them were classified as having a stable disease using RECIST 1.1 criteria.

Early T2* increases from baseline were observed for 3/4 non-responders and 3/6 responders, whereas T2* reductions were consistently observed post-RT for both response groups (Figure 3b).

Figure 3c–e demonstrate the significantly lower median vascular parameters for non-responders at baseline (Table 2). Early reductions from baseline for parameters reflecting contrast agent uptake ((Gd), IAUGC60) were demonstrated for the majority of responding tumours, whereas, most non-responding tumours showed early uptake increases. Contrary to our expectations, (Gd) and IAUGC60 were not significantly correlated.

In assessment of median K^{trans} changes, overall reductions and increases from baseline were consistently observed among responders and non-responders respectively. One responder exhibited an initial increase in median IAUGC60 and K^{trans} but a steep decrease in these parameters followed (Figure 3d and e, double red arrow). A significant positive correlation was demonstrated between K^{trans} and IAUGC60 (r = 0.59, p = 0.0013) but all other parameter associations did not reach statistical significance (p > 0.05).

DISCUSSION

In this descriptive study, we analyse the evolution of MRI-derived functional parameters in a uniform cohort of MLS patients from the DOREMY clinical trial. We have described early and late tumour functional changes seen with MRI.

MLS could be indistinguishable from cystic lesions and other soft-tissue masses using conventional MRI.[30,31] However, unlike cysts, MLS in this cohort showed marked contrast uptake in agreement with previous reports[31–33] and gradual enhancement potentially resulting from the myxomatous large interstitial compartments and fibrous tissue within MLS.[32,34] The slow gradual enhancement observed (Supplementary Figure 1) was a characteristic for all MLS in our cohort and therefore we expect the vascular parameters to be the most relevant to study response.

The baseline ADC values in the present study are higher than the values reported previously, due to the myxoid matrix of MLS.[35] The baseline ADC values and their post-treatment changes were not different between the two response groups. STS may have areas of fat, necrosis, viable tumour and haemorrhage with different diffusion properties[36] suggesting that tissue integration may obscure ADC changes with treatment. ADC increases post-RT observed in two responding patients assessed as having stable disease by RECIST 1.1 criteria is in broad agreement with a study by Winfield et al.[37]

T2* relaxation time is an imaging biomarker that has shown an association with tumour oxygenation as well as a dependency on tissue structure.[38–41] Our observations support T2* dependency on tissue structure; tumours with different tissue content exhibited different T2* change behaviour (Figure 3). The wide range of T2* baseline values found is indicative of the inter- and

Figure 3. Graphs showing the median parameter estimates and the corresponding median absolute deviation for each patient separately at visit 1, visit 2 and the post-RT visit. A steep decrease in ADC post-RT (a, single black arrow) corresponds to a small change in T2* across visits (b, single black arrow) for a mass with 40% viable tumour, 30% necrosis and high fat content. A steep early T2* decrease corresponds to a mass showing residual viable tumour and fibrosis (b, double black arrow). A steep reduction of (Gd) post-RT (c, single red arrow) corresponds to a mass with a reported prominent capillary vasculature. The same pattern was not observed in IAUGC60 which increased between these two visits (d, single red arrow). Number of patients considered in each graph: ADC (n_resp = 6, n_nresp = 4), T2* (n_resp = 6, n_nresp = 4), (Gd)/IAUGC60 (n_resp = 6, n_nresp = 3, one non-responder did not receive contrast agent), K^{trans} (n_resp = 5, n_nresp = 3, baseline K^{trans} was considered non-reliable for one responder and therefore the patient was excluded from the graph, one non-responder did not receive contrast agent), volume (n_resp = 6, n_nresp = 4). ADC, apparent diffusion coefficient.

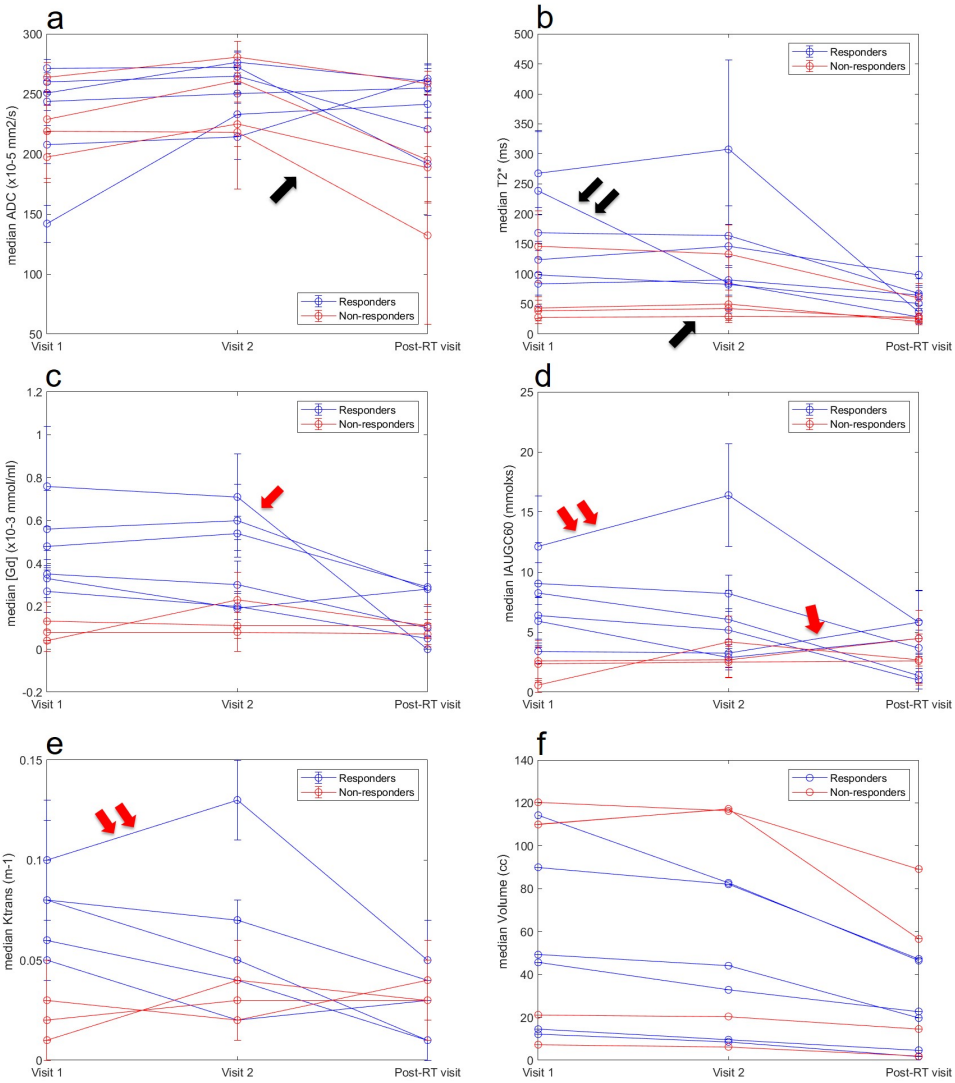

intratumoral heterogeneity of MLS in this cohort. Low T2* variability among MLS have been previously reported,[42] however, measurements concern a central slice excluding areas of necrosis and haemorrhage. Our observation of statistically significant T2* decreases post-RT for responders is potentially related to treatment-induced fibrosis[38] and sclerosis. Non-responding tumours exhibited lower baseline T2* values and therefore there has less scope for a proportional T2* reduction post-RT compared to the responding tumours.

The baseline values of the quantitative vascular MRI parameters reported herein show promise in the prediction of treatment response. Baseline K^{trans} has been previously found to be a good marker for the prediction of early soft-tissue sarcoma response.[17] Our findings suggest that MLS with higher perfusion and permeability at baseline have higher blood supply indicating better oxygenation, and therefore greater radiosensitivity[43] and better response. In contrast, Huang et al[17] found lower baseline perfusion and permeability for optimally responding tumours, however, the soft-tissue sarcoma patient cohort was heterogeneous and subtypes assessments were not performed. Decreases of K^{trans} early in the RT course and post-RT of the responding tumours agree with other DCE-MRI clinical and pre-clinical studies of soft-tissue sarcomas.[17,18,44,45] The increase of K^{trans} in

the non-responding tumours may relate to underline functions that support increased perfusion for future growth.[18]

IAUGC60 and model-based K^{trans} show an association for all patients (Figure 3d and e) and this observation agrees with previous studies reporting strong correlations between the two parameters.[38,46] Therefore, IAUGC60 is often the parameter of choice clinically due to its robustness and lack of assumptions. However, simulations performed by Walker-Samuel et al[46] revealed that IAUGC is a mixed metric and should not be used as a surrogate measure of K^{trans}.

Similar to IAUGC60, baseline (Gd) was able to discriminate response. In contrast to pharmacokinetic modelling, (Gd) measurement for delayed contrast-agent uptake is a simple and easy method to implement; it relies on T1 measurements and avoids challenges associated with rapid acquisitions and modelling.

Against our expectation, we did not find an association between (Gd) and IAUGC60 and therefore several sources of measurement error were considered. Flip angle accuracy is of paramount importance in determining the accuracy of quantitative DCE-MRI. It affects the baseline T1 and hence the calculation of the contrast agent uptake and vessel permeability. Flip angle non-uniformities arise from B1 inhomogeneities which are more pronounced at large magnetic fields (≥3T) and large FOV.[22] In the present study, we corrected our DCE-MRI quantitative measurements over the ROI by applying a scaling factor to the flip angle derived using the signal from fat as a reference.

DCE-MRI parameter estimations may be affected by blood inflow, and these effects cannot be completely excluded in this cohort. Other potential sources of error (non-steady state of the longitudinal magnetisation, receiver gain changes between low and high flip angle acquisitions and adequacy of the spoiled GRE equation[47] to characterise our data) were examined and found that they are unlikely to have affected our T1 measurements.

Early volume changes were significantly different in responding MLS suggesting that RT-induced size reductions occur early within the treatment course. Opposite results were reported by Huang et al[17] but their cohort was heterogeneous comprising soft-tissue sarcomas of different histological subtypes. Large treatment-induced size reductions have been reported for MLS in several studies[13,48,49] and the response has been related to tumour volume changes.[13]

There were limitations to the study. First, the sample size of the cohort is small, but constitutes a homogenous patient population. Nevertheless this study contributes important information, as only a limited body of literature assesses the value of functional MRI in discriminating STS response to radiotherapy, and none of those studies are dedicated to a uniform cohort of MLS. In addition, small studies like ours aim to create further hypothesis to be tested in larger studies. The observation of no significant changes of ADC could be attributed to the small sample size and also the fact that all parameters were calculated including the entire tumour volume considered. A more sophisticated analysis excluding areas of necrosis and fat could potentially prove useful in highlighting the value of ADC in discriminating response of MLS as suggested in other STS studies.[19,36,37,50] Another limitation of the study is the lack of repeatability evaluation for the parameters considered. However, good ADC, T2*, IAUGC60 and K^{trans} repeatability has been demonstrated in previous reports suggesting the implementation of such parameters with a high level of confidence.[27,37,51,52] We acknowledge there are risks associated with the administration of multiple doses of Gd-based contrast agents (nephrogenic systemic fibrosis and retention in a range of tissues and organs). However, all patients received contrast agent in our cohort were administered a macrocyclic Gd-based contrast agent where the risks are much lower compared to their linear counterparts.[53] Moreover, all individuals were at a low risk of an adverse event and therefore, the cohort was expected to experience no risks in addition to those for standard MRI scanning with administration of Gd-based contrast agent.

In conclusion, in this pilot study we have described functional changes in a homogenous cohort of MLS patients receiving reduced dose RT. Vascular parameters (Pre-treatment (Gd), IAUGC60 and K^{trans}) were significantly higher for responders and their predictive value merits further investigation. MLS are heterogenous lesions, characterised by a slow gradual contrast-agent uptake. The delayed (Gd) is a suitable descriptive parameter, relying simply on T1 measurements pre- and post-contrast agent injection. Early changes to tumour volume, vascular parameters ((Gd), IAUGC60 and K^{trans}) and T2* have potential in identifying response to treatment. Further work is required to describe tumour heterogeneity and ensure functional differences are not obscured by integration of functional parameters over the tumour volume.

ACKNOWLEDGEMENTS

We acknowledge funding from Cancer Research UK and Engineering and Physical Sciences Research Council support to the Cancer Imaging Centre at the Institute of Cancer Research and Royal Marsden Hospital in association with the Medical Research Council and Department of Health C1060/A10334, C1060/A16464 and National Health Service funding to the National Institute for Health Research Biomedical Research Centre, Experimental Cancer Medicine Centre, the Clinical Research Facility in Imaging, and the Cancer Research Network. The views expressed in this publication are those of the author(s) and not necessarily those of the National Health Service, the National Institute for Health Research or the Department of Health.

REFERENCES

1. Pitson G, Robinson P, Wilke D, Kandel RA, White L, Griffin AM, et al. Radiation response: an additional unique signature of myxoid liposarcoma. *Int J Radiat Oncol Biol Phys* 2004; **60**: 522–6. doi: https://doi.org/10.1016/j.ijrobp.2004.03.009
2. de Vreeze RSA, de Jong D, Haas RL, Stewart F, van Coevorden F. Effectiveness of radiotherapy in myxoid sarcomas is associated with a dense vascular pattern. *Int J Radiat Oncol Biol Phys* 2008; **72**: 1480–7. doi: https://doi.org/10.1016/j.ijrobp.2008.03.008
3. Chung PWM, Deheshi BM, Ferguson PC, Wunder JS, Griffin AM, Catton CN, et al. Radiosensitivity translates into excellent local control in extremity myxoid liposarcoma: a comparison with other soft tissue sarcomas. *Cancer* 2009; **115**: 3254–61. doi: https://doi.org/10.1002/cncr.24375
4. Guadagnolo BA, Zagars GK, Ballo MT, Patel SR, Lewis VO, Benjamin RS, et al. Excellent local control rates and distinctive patterns of failure in myxoid liposarcoma treated with conservation surgery and radiotherapy. *Int J Radiat Oncol Biol Phys* 2008; **70**: 760–5. doi: https://doi.org/10.1016/j.ijrobp.2007.07.2337
5. Moser EC, Noordijk EM, van Leeuwen FE, le Cessie S, Baars JW, Thomas J, et al. Long-term risk of cardiovascular disease after treatment for aggressive non-Hodgkin lymphoma. *Blood* 2006; **107**: 2912–9. doi: https://doi.org/10.1182/blood-2005-08-3392
6. Venkatesulu BP, Mahadevan LS, Aliru ML, Yang X, Bodd MH, Singh PK, et al. Radiation-induced endothelial vascular injury: a review of possible mechanisms. *JACC Basic Transl Sci* 2018; **3**: 563–72. doi: https://doi.org/10.1016/j.jacbts.2018.01.014
7. Yusuf W, Venkatesulu BP, Mahadevan LS, Krishnan S. Radiation-Induced cardiovascular disease: a clinical perspective Syed. radiation-induced cardiovascular disease: a clinical perspective. *Front Cardiovasc Med* 2017; **4**: 66.
8. Friedman M, Egan JW. Irradiation of liposarcoma. *Acta radiol* 1960; **54**: 225–39. doi: https://doi.org/10.3109/00016926009172544
9. Lansu J, Bovée JVMG, Braam P, van Boven H, Flucke U, Bonenkamp JJ, et al. Dose reduction of preoperative radiotherapy in myxoid liposarcoma. *JAMA Oncology* 2021; **7**: e205865. doi: https://doi.org/10.1001/jamaoncol.2020.5865
10. Shapeero LG, Vanel D, Verstraete KL, Bloem JL. Fast magnetic resonance imaging with contrast for soft tissue sarcoma viability. *Clin Orthop Relat Res* 2002; **397**: 212–27. doi: https://doi.org/10.1097/00003086-200204000-00026
11. Soldatos T, Ahlawat S, Montgomery E, Chalian M, Jacobs MA, Fayad LM. Multiparametric assessment of treatment response in high-grade soft-tissue sarcomas with anatomic and functional MR imaging sequences. *Radiology* 2016; **278**: 831–40. doi: https://doi.org/10.1148/radiol.2015142463
12. Canter RJ, Martinez SR, Tamurian RM, Wilton M, Li C-S, Ryu J, et al. Radiographic and histologic response to neoadjuvant radiotherapy in patients with soft tissue sarcoma. *Ann Surg Oncol* 2010; **17**: 2578–84. doi: https://doi.org/10.1245/s10434-010-1156-3
13. Roberge D, Skamene T, Nahal A, Turcotte RE, Powell T, Freeman C. Radiological and pathological response following pre-operative radiotherapy for soft-tissue sarcoma. *Radiother Oncol* 2010; **97**: 404–7. doi: https://doi.org/10.1016/j.radonc.2010.10.007
14. Padhani AR, Miles KA. Multiparametric imaging of tumor response to therapy. *Radiology* 2010; **256**: 348–64. doi: https://doi.org/10.1148/radiol.10091760
15. Leach MO, Morgan B, Tofts PS, Buckley DL, Huang W, Horsfield MA. Experimental cancer medicine centres imaging network Steering Committee. imaging vascular function for early stage clinical trials using dynamic contrast-enhanced magnetic resonance imaging. *Eur Radiol* 2012; **22**: 1451–64.
16. Klaassen R, Gurney-Champion OJ, Wilmink JW, Besselink MG, Engelbrecht MRW, Stoker J, et al. Repeatability and correlations of dynamic contrast enhanced and T2* MRI in patients with advanced pancreatic ductal adenocarcinoma. *Magn Reson Imaging* 2018; **50**: 1–9. doi: https://doi.org/10.1016/j.mri.2018.02.005
17. Huang W, Beckett BR, Tudorica A, Meyer JM, Afzal A, Chen Y, et al. Evaluation of soft tissue sarcoma response to preoperative chemoradiotherapy using dynamic contrast-enhanced magnetic resonance imaging. *Tomography* 2016; **2**: 308–16. doi: https://doi.org/10.18383/j.tom.2016.00202
18. Spratt DE, Arevalo-Perez J, Leeman JE, Gerber NK, Folkert M, Taunk NK, et al. Early magnetic resonance imaging biomarkers to predict local control after high dose stereotactic body radiotherapy for patients with sarcoma spine metastases. *Spine J* 2016; **16**: 291–8. doi: https://doi.org/10.1016/j.spinee.2015.08.041
19. Dudeck O, Zeile M, Pink D, Pech M, Tunn P-U, Reichardt P, et al. Diffusion-Weighted magnetic resonance imaging allows monitoring of anticancer treatment effects in patients with soft-tissue sarcomas. *J Magn Reson Imaging* 2008; **27**: 1109–13. doi: https://doi.org/10.1002/jmri.21358
20. Kousi E, O'Flynn EAM, Borri M, Morgan VA, deSouza NM, Schmidt MA. Pre-treatment functional MRI of breast cancer: T2* evaluation at 3 T and relationship to dynamic contrast-enhanced and diffusion-weighted imaging. *Magn Reson Imaging* 2018; **52**: 53–61. doi: https://doi.org/10.1016/j.mri.2018.05.014
21. Myronenko A. Medical image registration toolbox (mirt) for matlab. 2010. Available from: https://sites.google.com/site/myronenko/research/mirt.
22. Cheng H-LM, Wright GA. Rapid high-resolution T(1) mapping by variable flip angles: accurate and precise measurements in the presence of radiofrequency field inhomogeneity. *Magn Reson Med* 2006; **55**: 566–74. doi: https://doi.org/10.1002/mrm.20791
23. Sung K, Saranathan M, Daniel BL, Hargreaves BA. Simultaneous T1 and B1+ mapping using reference resion variable FLIP angle iaging. *Magn Reson Med* 2013; **70**: 1306–18.
24. Tofts PS, Brix G, Buckley DL, Evelhoch JL, Henderson E, Knopp MV, et al. Estimating kinetic parameters from dynamic contrast-enhanced T(1)-weighted MRI of a diffusable tracer: standardized quantities and symbols. *J Magn Reson Imaging* 1999; **10**: 223–32. doi: https://doi.org/10.1002/(sici)1522-2586(199909)10:3<223::aid-jmri2>3.0.co;2-s
25. Orton MR, d'Arcy JA, Walker-Samuel S, Hawkes DJ, Atkinson D, Collins DJ, et al. Computationally efficient vascular input function models for quantitative kinetic modelling using DCE-MRI. *Phys Med Biol* 2008; **53**: 1225–39. doi: https://doi.org/10.1088/0031-9155/53/5/005
26. Parker GJM, Roberts C, Macdonald A, Buonaccorsi GA, Cheung S, Buckley DL, et al. Experimentally-derived functional form for a population-averaged high-temporal-resolution arterial input function for dynamic contrast-enhanced MRI. *Magn Reson Med* 2006; **56**: 993–1000. doi: https://doi.org/10.1002/mrm.21066
27. Rata M, Collins DJ, Darcy J, Messiou C, Tunariu N, Desouza N. Assessment of repeatability and treatment response in early phase clinical trials using DCE-MRI: comparison of parametric analysis

using MR- and CT-derived arterial input functions. *Eur. Radiol* 1998; **2016**: 1991.
28. Ferl GZ, O'Connor JPB, Parker GJM, Carano RAD, Acharya SJ, Jayson GC. Mixed-Effects modeling of clinical DCE-MRI data: application to colorectal liver metastases treated with Bevacizumad. *JMR* 2015; **41**: 132–41.
29. Eisenhauer EA, Therasse P, Bogaerts J, Schwartz LH, Sargent D, Ford R. New response evaluation criteria in solid tumours: revised RECIST guideline (version 1.1). *Eur J Cancer* 2009; **45**: 228–47.
30. Landa J, Schwartz LH. Contemporary imaging in sarcoma. *The Oncologist* 2009; **14**: 1021–38.
31. Sung MS, Kang HS, Suh JS, Lee JH, Park JM, Kim JY. Myxoid liposarcoma: appearance at MR imaging with histologic correlation. *Radiographics* 2000; **20**: 1007–19.
32. Kim T, Murakami T, Oi H, Tsuda K, Matsushita M, Tomoda K. Ct and MR imaging of abdominal liposarcoma. *AJR Am J Roentgenol* 1996; **166**: 829–33.
33. Löwenthal D, Zeile M, Niederhagen M, Fehlberg S, Schnapauff D, Pink D. Differentiation of myxoid liposarcoma by magnetic resonance imaging: a histopathologic correlation. *Acta Radiol* 2014; **55**: 952–60.
34. Drape JL. Advances in magnetic resonance imaging of musculoskeletal tumour. *Orthopaedics & Traumatology: Surgery & Research* 2013; **99**: 115–23.
35. Maeda M, Matsumine A, Kato H, Kusuzaki K, Maier SE, Uchida A. Soft-Tissue tumors evaluated by line-scan diffusion-weighted imaging: influence of myxoid matrix on the apparent diffusion coefficient. *J Magn Reson Imaging* 2007; **25**: 1199–204.
36. Lang P, Wendland MF, Saeed M, Gindele A, Rosenau W, Mathur A. Osteogenic sarcoma: noninvasive in vivo assessment of tumor necrosis with diffusion-weighted MR imaging. *Radiology* 1998; **206**: 227–35.
37. Winfield JM, Miah AB, Strauss D, Thway K, Collins DJ, deSouza NM. Utility of multi-parametric quantitative magnetic resonance imaging for characterisation and radiotherapy response assessment in soft-tissue sarcomas and correlation with histopathology. *Front Oncol* 2019; **9**: 280.
38. SP L, Taylor NJ, Makris A, Ah-See MW, Beresford MJ, Stirling JJ. Primary human breast adenocarcinoma: imaging and histologic correlates of intrinsic susceptibility-weighted MR imaging before and during chemotherapy. *Radiology* 2010; **257**: 643–52.
39. Baudelet C, Gallez B. How does blood oxygen level-dependent (BOLD) contrast correlate with oxygen partial pressure (PO2) inside tumors? *Magn Reson Med* 2002; **48**: 980–6.
40. Zhao D, Jiang L, Hahn EW, Mason RP. Comparison of 1H blood oxygen level-dependent (BOLD) and 19F MRI to investigate tumor oxygenation. *Magn Reson Med* 2009; **62**: 357–64.
41. Chopra S, Foltz WD, Milosevic MF, Toi A, Bristow RG, Menard C. Comparing oxygen-sensitive MRI (BOLD R2*) with oxygen electrode measurements: a pilot study in men with prostate cancer. *Int J Radiat Biol* 2009; **85**: 805–13.
42. Nikiforaki K, Manikis GC, Kontopodis E, Lagoudaki E, de Breed E, Marias K. T2, T2* and spin coupling ratio as biomarkers for the study of lipomatous tumors. *Physica Medica* 2019; **60**: 76–82.
43. Cho H, Ackerstaff E, Carlin S, Lupu ME, Wanh Y, Rizwan A. Noninvasive multimodality imaging of tumor microenvironment: registered dynamic magnetic resonance imaging and positron emission tomography studies of a preclinical tumor model of tumor hypoxia. *Neoplasia* 2009; **11**: 247–59.
44. Preda A, Wielopolski PA, Ten Hagen TL, van Vliet M, Veenland JF, Ambagtsheer G. Dynamic contrast-enhanced MRI using macromolecular contrast media for monitoring the response to isolated limb perfusion in experimental soft-tissue sarcomas. *MAGMA* 2004; **17**: 296–302.
45. Alic L, van Vliet M, Wielopolski PA, ten Hagen TL, van Dijke CF, Niessen WJ. Regional heterogeneity changes in DCE-MRI as response to isolated limb perfusion in experimental soft-tissue sarcomas. *Contrast Media Mol Imaging* 2013; **8**: 340–9.
46. Walker-Samuel S, Leach MO, Collins DJ. Evaluation of response to treatment using DCE-MRI: the relationship between initial area under the gadolinium curve (IAUGC) and quantitative pharmacokinetic analysis. *Phys. Med. Biol* 2006; **51**: 3593–602.
47. Wang HZ, Riederer SJ, Lee JN. Optimizing the precision in T1 relaxation estimation using limited FLIP angles. *Magn Reson Med* 1987; **5**: 399–416.
48. Le Grange F, Cassoni AM, Seddon BM. The significance of size change of soft tissue sarcoma during preoperative radiotherapy. *EJSO* 2014; **40**: 394–401.
49. Rosenberg M, Groth JV, Taljanovic MS, Mar WA. Myxoid-round cell liposarcoma: MRI appearance after radiation therapy and relationship to response. *Radiol Case Rep* 2017; **12**: 811–4.
50. Einarsdottir H, Karlsson M, Wejde J, Bauer HCF. Diffusion-Weighted MRI of soft tissue tumours. *Eur Radiol* 2004; **14**: 959–63.
51. Messiou C, Orton M, Ang JE, Collins DJ, Morgan VA, Mears D. Advanced solid tumours treated with cediranib: comparison of dynamic contrast-enhanced MR imaging and CT as markers of vascular activity. *Radiology* 2012; **265**: 426–36.
52. Panek R, Welsh L, Dunlop A, Wong KH, Riddell AM, Koh DM. Repeatability and sensitivity of T2* measurements in patients with head and neck squamous cell carcinoma at 3T. *J Magn Reson Imaging* 2016; **44**: 72–80.
53. Royal College of Radiologists.2019. Guidance on Gadolinium-based contrast agent administration to adult patients